Article

Current Biology

The Antiviral RNA Interference Response Provides Resistance to Lethal Arbovirus Infection and Vertical Transmission in *Caenorhabditis elegans*

Highlights

- *C. elegans* can be infected by vesicular stomatitis virus through microinjection
- The antiviral RNAi pathway restricts infection to muscle tissue and prolongs survival
- The antiviral RNAi pathway also serves to prevent vertical transmission of viruses
- Resistance to infection by vesicular stomatitis virus is heritable in *C. elegans*

Authors

Don B. Gammon, Takao Ishidate, Lichao Li, Weifeng Gu, Neal Silverman, Craig C. Mello

Correspondence

don.gammon@utsouthwestern.edu (D.B.G.), craig.mello@umassmed.edu (C.C.M.)

In Brief

Gammon, Ishidate, et al. report that vesicular stomatitis virus produces a lethal infection in *C. elegans*. The nematode RNA interference pathway restricts infection to muscle tissue, inhibits vertical transmission, and promotes transgenerational inheritance of antiviral immunity. This study establishes a promising system for exploring virus-host interplay.

Gammon et al., 2017, Current Biology *27*, 795–806
March 20, 2017 © 2017 The Authors. Published by Elsevier Ltd.
http://dx.doi.org/10.1016/j.cub.2017.02.004

CellPress

Current Biology
Article

The Antiviral RNA Interference Response Provides Resistance to Lethal Arbovirus Infection and Vertical Transmission in *Caenorhabditis elegans*

Don B. Gammon,[1,5,6,*] Takao Ishidate,[1,2,5] Lichao Li,[3] Weifeng Gu,[3] Neal Silverman,[4] and Craig C. Mello[1,2,7,*]
[1]RNA Therapeutics Institute, University of Massachusetts Medical School, Worcester, MA 01605, USA
[2]Howard Hughes Medical Institute, University of Massachusetts Medical School, Worcester, MA 01605, USA
[3]Department of Cell Biology and Neuroscience, University of California, Riverside, Riverside, CA 92521, USA
[4]Department of Medicine, University of Massachusetts Medical School, Worcester, MA 01605, USA
[5]Co-first author
[6]Present address: Department of Microbiology, University of Texas Southwestern Medical Center, Dallas, TX 75390, USA
[7]Lead Contact
*Correspondence: don.gammon@utsouthwestern.edu (D.B.G.), craig.mello@umassmed.edu (C.C.M.)
http://dx.doi.org/10.1016/j.cub.2017.02.004

SUMMARY

The recent discovery of the positive-sense single-stranded RNA (ssRNA) Orsay virus (OV) as a natural pathogen of the nematode *Caenorhabditis elegans* has stimulated interest in exploring virus-nematode interactions. However, OV infection is restricted to a small number of intestinal cells, even in nematodes defective in their antiviral RNA interference (RNAi) response, and is neither lethal nor vertically transmitted. Using a fluorescent reporter strain of the negative-sense ssRNA vesicular stomatitis virus (VSV), we show that microinjection of VSV particles leads to a dose-dependent, muscle tissue-tropic, lethal infection in *C. elegans*. Furthermore, we find nematodes deficient for components of the antiviral RNAi pathway, such as Dicer-related helicase 1 (DRH-1), to display hypersusceptibility to VSV infection as evidenced by elevated infection rates, virus replication in multiple tissue types, and earlier mortality. Strikingly, infection of oocytes and embryos could also be observed in *drh-1* mutants. Our results suggest that the antiviral RNAi response not only inhibits vertical VSV transmission but also promotes transgenerational inheritance of antiviral immunity. Our study introduces a new, in vivo virus-host model system for exploring arbovirus pathogenesis and provides the first evidence for vertical pathogen transmission in *C. elegans*.

INTRODUCTION

Genetic tractability, ease of culture, and susceptibility to a variety of bacterial and fungal pathogens [1, 2] have made *C. elegans* attractive for exploring microbe-host interactions. However, due to a lack of convenient experimental systems, relatively few studies have explored virus-*C. elegans* interactions. Initial studies investigating virus-*C. elegans* interactions used primary cell cultures and defined an antiviral role for the nematode RNA interference (RNAi) response [3, 4].

RNAi is a highly conserved mechanism of gene silencing that contributes to antiviral defense in insects [5], plants [6], and mammals [7, 8]. In *C. elegans*, the antiviral RNAi response is initiated after recognition and cleavage of viral double-stranded RNAs by a complex consisting of Dicer-related helicase 1 (DRH-1), DCR-1, and RDE-4 into 23-nt-long primary small interfering RNAs (siRNAs) [9]. These duplex siRNAs are then loaded into the primary Argonaute protein RDE-1 and one strand of the duplex is lost. These RDE-1-primary siRNA complexes then recruit RNA-dependent RNA polymerase complexes to viral RNA targets, where they generate secondary siRNAs termed "22Gs," which are typically 22 nt long and contain 5′ guanines [10, 11]. These 22Gs then complex with, and guide, secondary Argonautes to complementary viral single-stranded RNA (ssRNA) targets (e.g., mRNAs or genomes), resulting in Argonaute-mediated target cleavage and inhibition of virus replication [9].

Despite initial insights into virus-*C. elegans* interactions provided by primary cell-culture studies, these cultures have limited utility because they are technically challenging to generate and may not be representative of infection in animals. To investigate virus-*C. elegans* interactions in vivo, Lu et al. created a nematode strain encoding a flock house virus replicon [12]. Although this replicon system has identified host factors, such as DRH-1 [13], that restrict virus replication, it cannot identify nematode factors influencing aspects of the viral life cycle that would only be afforded with a bona fide viral pathogen (e.g., transmission, entry, exit, etc.) [14].

More recently, the positive-sense ssRNA Orsay virus (OV) was described as a natural pathogen of *C. elegans* [14]. The discovery of OV represents an important step in defining virus-nematode interactions; however, this model also possesses limitations. First, OV infection is limited to one to six intestinal cells, even during infection of RNAi-deficient animals [15]. Therefore, identifying antiviral factors specific to non-intestinal tissues with the OV model may be difficult. Second, because OV infection is not lethal [14], scoring the minor pathological features of infection can be challenging. Third, recombinant OV strains expressing

This is an open access article under the CC BY-NC-ND license (http://creativecommons.org/licenses/by-nc-nd/4.0/).

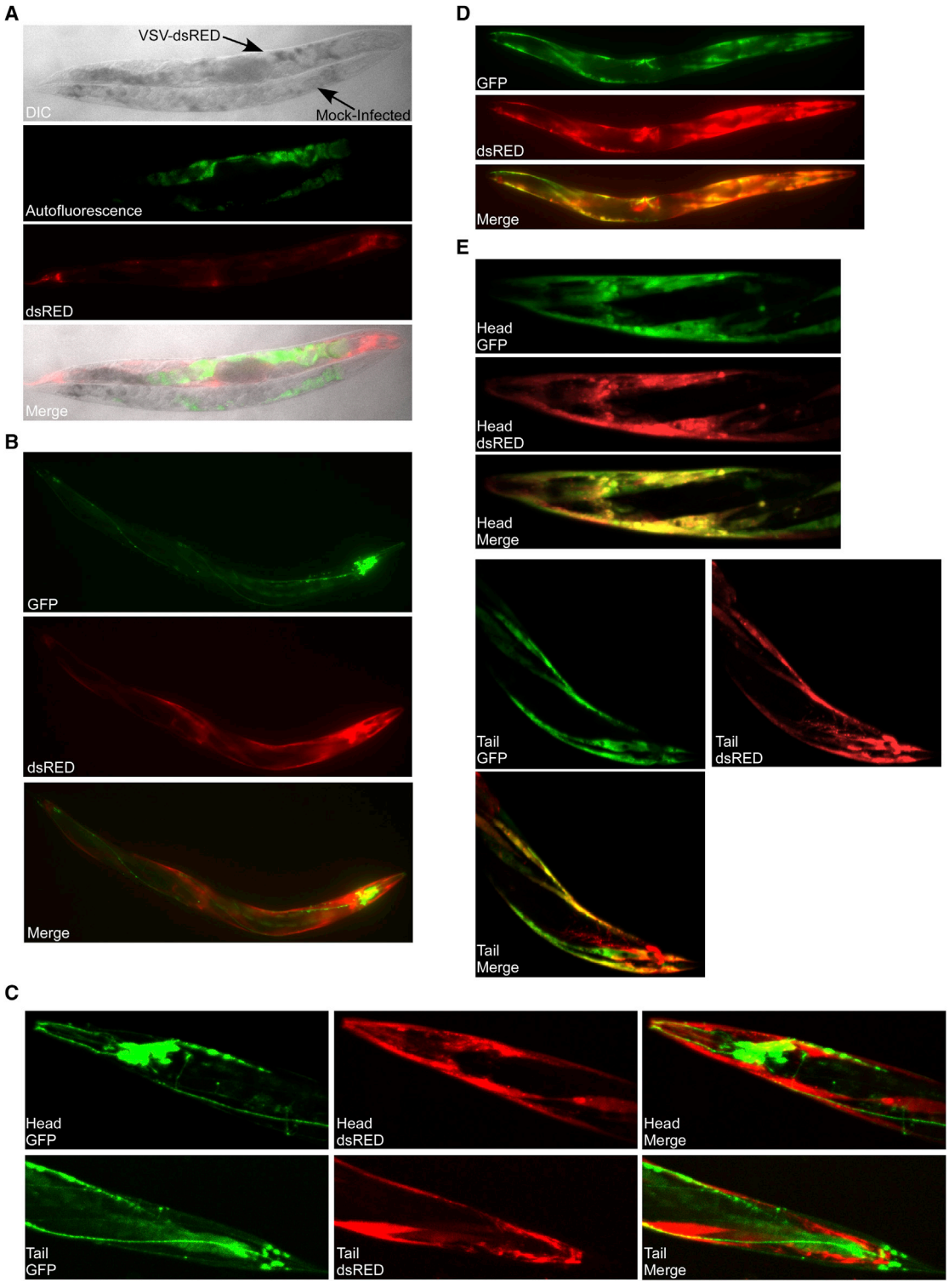

Figure 1. Microinjection of Adult *C. elegans* Animals with Recombinant VSV Expressing dsRED Results in an Infection Primarily Restricted to Muscle Tissue

(A) Differential interference contrast (DIC) and fluorescence micrographs (10× magnification) of N2 adults either mock or VSV-dsRED infected. Images were taken 72 hr post-infection (hpi). Green fluorescence indicates autofluorescence signal in the intestine.

(B) Fluorescence micrographs (10× magnification) of a p*sng-1*::LUC-GFP adult infected with VSV-dsRED 72 hpi.

(legend continued on next page)

fluorescent or quantifiable reporter genes are unavailable, making analysis of OV replication limited to PCR- or immunofluorescence-based methods. Finally, because OV is not vertically transmitted [14], this model may be unsuitable for identifying immunity mechanisms guarding against vertical transmission.

Given the shortcomings of current virus-*C. elegans* model systems, we asked whether an alternative system could be established using the negative-sense ssRNA vesicular stomatitis virus (VSV). VSV is a member of the arboviruses, a group of emerging viral pathogens that are transmitted by arthropods to vertebrate hosts. The wide availability of reverse genetic and immunological tools for VSV [16, 17] makes it convenient for studying arboviral disease mechanisms relevant to human and animal health [18, 19]. Furthermore, because VSV can replicate in *C. elegans* primary cells [3, 4], we thought it possible that VSV could infect *C. elegans* animals.

Here we show that microinjection of VSV particles produces a lethal infection in *C. elegans*. We further show that the susceptibilities of animals to infection, the tissues infected, and animal survival are dependent upon virus dose, culturing conditions, and host genetic background. We also establish a role for the nematode antiviral RNAi pathway in restricting arbovirus replication and pathogenesis. Finally, we use this model to provide the first evidence for vertical transmission in *C. elegans* and implicate the antiviral RNAi response in both inhibiting vertical transmission and promoting transgenerational inheritance of antiviral immunity.

RESULTS

Microinjection of VSV into *C. elegans* Results in an Infection Primarily Restricted to Muscle Tissue

To determine whether VSV could infect *C. elegans*, we microinjected wild-type (N2 strain) adults with a recombinant VSV strain encoding the fluorescent reporter dsRED (VSV-dsRED) [20]. We targeted the body cavity and intestinal tissue just posterior to the terminal bulb of the pharynx for injections. After microinjection, we observed a prominent dsRED signal in animals that was both above background signals in mock-infected animals and significantly different from autofluorescence observed in intestinal tissues (Figure 1A). Microinjection of VSV-dsRED into transgenic animals expressing GFP under a neuronal promoter [21] revealed only a minor overlap of GFP and dsRED signals in head neurons (Figures 1B and 1C). However, significant overlap in dsRED and GFP signals was observed throughout infected transgenic animals expressing GFP under a muscle-specific promoter [21] (Figure 1D), with clear infection of body wall muscle in the head and tail (Figure 1E). We could also establish VSV-dsRED infections in the Hawaiian isolate (CB4856) of *C. elegans* (Figure S1A) and in *Caenorhabditis briggsae* (Figure S1B). Interestingly, whereas both the N2 and Hawaiian animals displayed infection rates of 85%–90%, only ~20% of *C. briggsae* animals displayed dsRED signal by 72 hr post-infection (hpi), suggesting that *C. briggsae* may be more resistant to infection (Figure S1C).

Loss of DRH-1 Function Results in Hypersusceptibility to Lethal VSV Infection

Previous flock house virus replicon [13] and OV [9] studies have implicated DRH-1 in the restriction of positive-sense ssRNA virus replication in *C. elegans*. DRH-1 functions in a similar manner as homologous mammalian RIG-I-like helicases (RLHs), which sense cytosolic viral RNA signatures and subsequently trigger antiviral response programs [9, 22]. Although mammalian RLHs and DRH-1 both trigger an antiviral response upon viral RNA recognition, mammalian RLHs trigger the interferon response [23], whereas DRH-1 promotes the initiation of the *C. elegans* antiviral RNAi response [9, 13].

To determine whether DRH-1 is involved in sensing negative-sense ssRNA virus infection, we challenged animals carrying a loss-of-function mutation in *drh-1* with VSV-dsRED and compared the dsRED pattern to N2 infections. Interestingly, *drh-1* worms displayed infection in multiple tissues not involved in N2 infections, such as intestinal tissue (Figure 2A). To further compare dsRED signals in N2 and *drh-1* strains, we microinjected either a low (10^2 plaque-forming units [PFU]) or high (10^4 PFU) dose of VSV-dsRED into either strain and then measured signals in either whole animals (Figure 2B) or specific tissues (Figures 2C–2F) 48 hpi. Whole-body dsRED measurements indicated that *drh-1* animals displayed ~5- and 18-fold higher signals than mock-infected animals at the 10^2 and 10^4 PFU doses, respectively. In contrast, dsRED signals in N2 animals were either essentially identical to or ~3-fold higher than mock-infected animals at these respective doses (Figure 2B). Measurement of dsRED signals in individual tissues revealed a similar pattern, with *drh-1* animals presenting with ~4- to 10-fold higher signals at the 10^2 PFU dose and ~17- to 51-fold higher signals at the 10^4 PFU dose compared to mock-infected animals. Significant N2 dsRED signals were typically only observed with 10^4 PFU treatments and were ~3- to 7-fold higher than mock-infected animals. Animals were scored as infected if their whole-body dsRED signals were at least 2-fold higher than mock-infected animals by 48 hpi. Using this cutoff, we found that at a dose of 10^4 PFU, 100% of both N2 and *drh-1* animals scored as infected. In contrast, no N2 and 80% of *drh-1* animals scored as infected in 10^2 PFU treatments (Figure 2G). However, when only vulval tissue dsRED signals were used to score infection in 10^2 PFU treatments, ~30% of N2 animals scored as infected (Figure S2), suggesting that this tissue may be a more reliable indicator of low-level infections. These results suggest that higher viral doses allow for viral replication to reach a threshold at which dsRED signals become detectable by 48 hpi in both N2 and *drh-1* strains. However, at lower viral doses, N2 animals may be more capable of suppressing VSV-dsRED replication and hence are not scored as infected by 48 hpi. Importantly, we confirmed that the elevated dsRED signal observed in *drh-1* animals reflected bona fide VSV transcription using RT-PCR (Figure S3) [24].

To examine viral susceptibilities of N2 and *drh-1* strains further, we tracked animals that had been microinjected with

(C) Confocal microscopy fluorescence micrographs (20× magnification) of head and tail regions of a p*sng-1*::GFP-LUC adult infected with VSV-dsRED 72 hpi.
(D) Fluorescence micrographs (10× magnification) of a p*myo-3*::LUC-GFP adult infected with VSV-dsRED 72 hpi.
(E) Confocal microscopy fluorescence micrographs (20× magnification) of head and tail regions of a p*myo-3*::GFP-LUC adult infected with VSV-dsRED 72 hpi.
All infections were carried out using 10^4 plaque-forming units (PFU) of VSV-dsRED per injection. See also Figure S1.

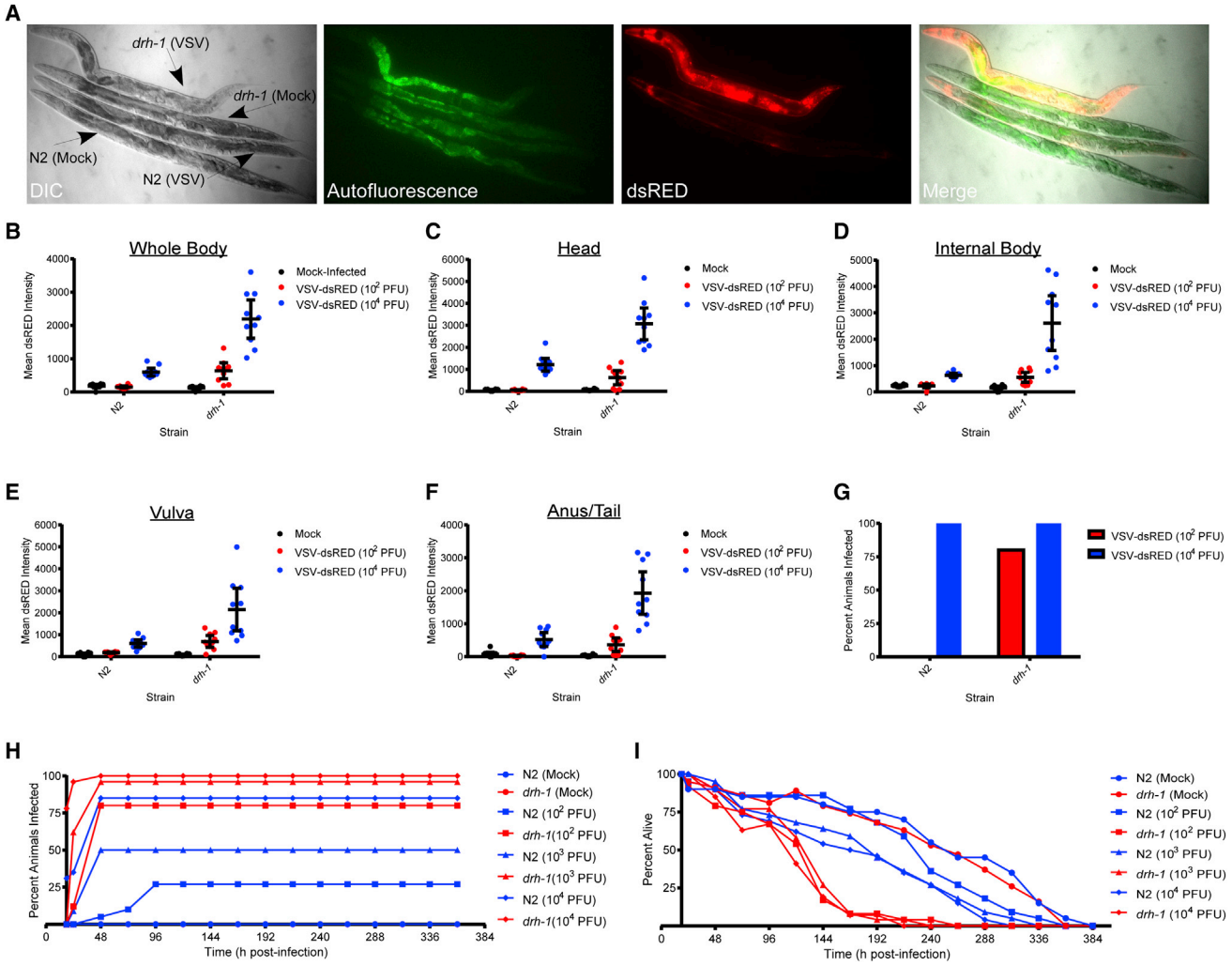

Figure 2. Loss of DRH-1 Function Results in Enhanced Susceptibility to VSV-dsRED Infection

(A) DIC and fluorescence micrographs (10× magnification) of N2 or *drh-1* adults mock infected or infected with 10^4 PFU of VSV-dsRED. Images were taken 72 hpi. Green fluorescence indicates autofluorescence obtained in the intestine.

(B–F) Mean dsRED intensity measurements for N2 or *drh-1* adults (n = 10/treatment) 48 hpi using the indicated VSV-dsRED dose. Measurements were taken of either the whole body (B) or the indicated tissues (C–F). Mean dsRED measurements for the entire group (horizontal bars) and 95% confidence intervals (error bars) are shown.

(G) Percentage of animals displaying a whole-body dsRED signal at least 2-fold above mock-infected animals by 48 hpi.

(H) Percentage of animals (n = 20–30/treatment) displaying dsRED signal at the indicated times post-infection.

(I) Percentage of animals from (H) alive at the indicated times post-infection.

See also Figures S2 and S3.

10^2, 10^3, or 10^4 PFU of VSV-dsRED for infection rate (Figure 2H) and survival (Figure 2I). The maximal number of infected animals in each injected group was reached by 48 hpi, with the exception of N2 animals injected with 10^2 PFU, which took until 96 hpi (Figure 2H). The 10^2, 10^3, and 10^4 PFU doses resulted in infection of 25%, 50%, and 85% of N2 animals, respectively. In contrast, these doses resulted in 80%, 95%, and 100% infection rates in *drh-1* animals (Figure 2H). Given that infection rates in several treatments never achieved 100%, it is likely that horizontal transmission of VSV between adults is inefficient.

We used lifespan assays (Figure 2I) to estimate the time at which 50% of animals in each treatment had died (expressed as lethal time 50 [LT_{50}] in hpi). We also calculated 95% confidence intervals (CIs) for each LT_{50} and, in cases where 95% CIs of two different LT_{50} values did not overlap, these two values were deemed statistically different ($p < 0.05$). The LT_{50} (95% CI) for mock-infected N2 animals (250 hpi [236–265 hpi]) was not significantly different from mock-infected *drh-1* mutants (240 hpi [228–252 hpi]). However, both N2 and *drh-1* animals had significantly lower LT_{50} values when infected with VSV-dsRED at any of the three doses used, suggesting that VSV infection is ultimately lethal. However, N2 animals survived for significantly longer periods of time than *drh-1* animals injected with the same viral dose. For example, at a dose of 10^2 PFU, the LT_{50} (95% CI) for N2 animals was 220 hpi (210–228 hpi) versus 112 hpi (104–119 hpi) for *drh-1* animals. This trend was

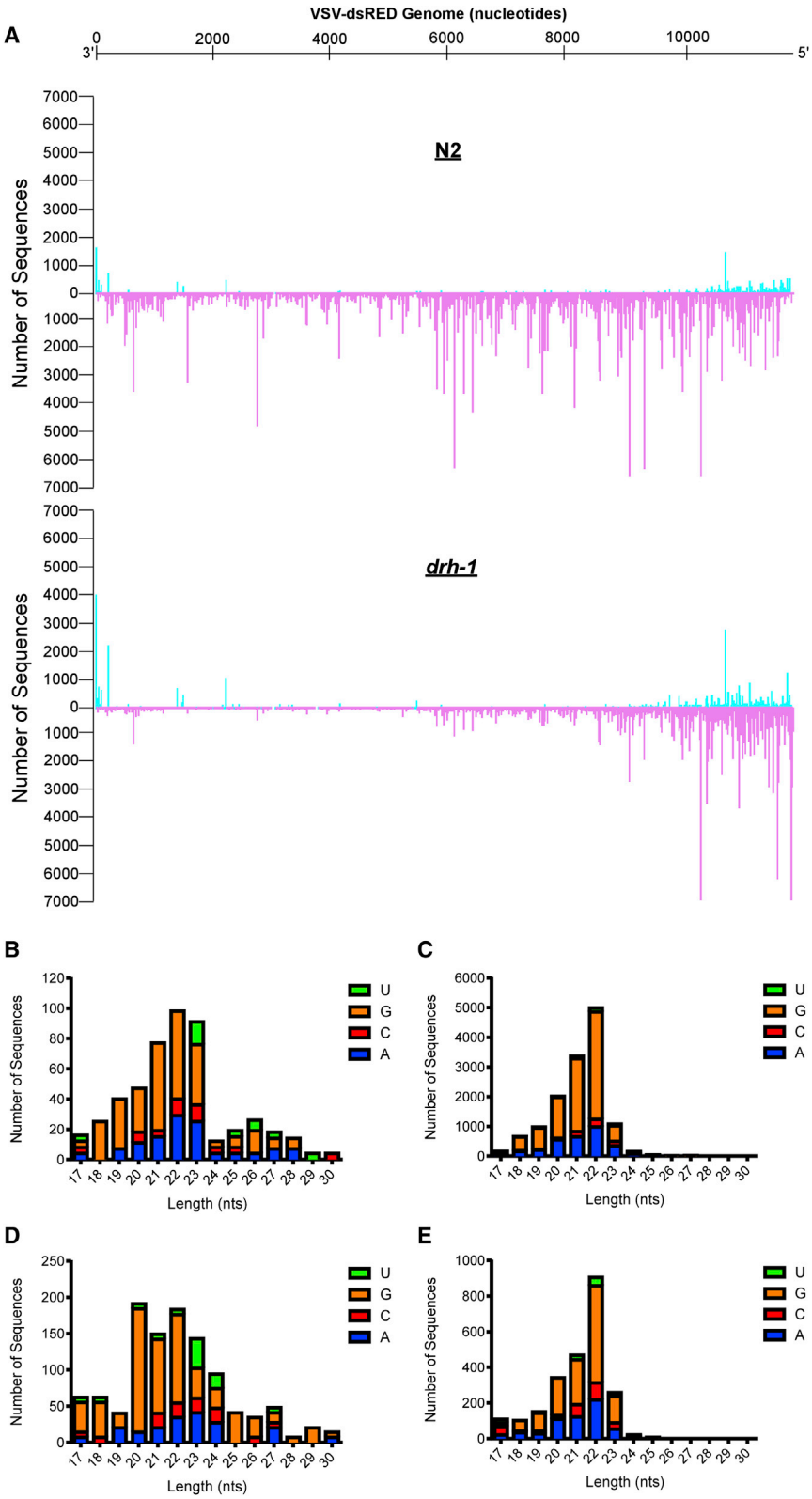

Figure 3. Small RNAs Produced upon VSV-dsRED Infection of N2 and *drh-1* Animals

(A) The number of unique sequences obtained by Illumina high-throughput small RNA sequencing that match a given position in the VSV-dsRED genome in infected N2 or *drh-1* animals is shown. The number of unique sequences in sense and antisense orientation is shown on the positive (cyan) and negative (purple) y axis, respectively. The negative-sense ssRNA VSV-dsRED genome (in 3′-to-5′ orientation) is depicted above.

(B and C) Features of sense (B) and antisense (C) small RNAs (length and identity of the first nucleotide) cloned from VSV-dsRED-infected N2 animals.

(D and E) Features of sense (D) and antisense (E) small RNAs cloned from VSV-dsRED-infected *drh-1* animals.

also observed at the 10^3 PFU dose, with LT_{50} (95% CI) for N2 animals being 176 hpi (166–186 hpi) versus 121 hpi (116–127 hpi) for *drh-1* animals and at the 10^4 PFU dose (N2, 168 hpi [162–174 hpi] versus *drh-1*, 106 hpi [99–112 hpi]). These results suggest that *drh-1* animals suffer higher infection rates and reduced survival times compared to N2 animals.

A Small RNA Response Is Generated upon VSV Infection

We next used deep sequencing to determine whether small RNAs (17–30 nt in length) were generated in response to VSV-dsRED infection. Small RNAs that mapped to the VSV-dsRED genome are shown in Figure 3A. These RNAs were virtually absent from uninfected animals (data not shown). In N2 libraries, small RNAs corresponding to the antisense (or genomic) strand of VSV-dsRED were ~29-fold more abundant than those mapping to the sense (antigenomic) strand (Figures 3B and 3C). Both antisense and sense RNAs were characterized by a peak length of 22 nt and a strong preference for G at their 5′ ends, and thus likely represent 22Gs. Consistent with a defect in the initiation of an antiviral RNAi response, ~4-fold fewer viral small RNAs were detected in *drh-1* animals than in N2 infections. Furthermore, although both antisense and sense small RNAs from *drh-1* animals also displayed a bias for 5′ G residues, a clear 22 nt peak length was only observed among antisense small RNAs (Figures 3D and 3E). In addition, *drh-1* antisense small RNAs were only 2-fold more abundant than sense RNAs. These results suggest that both N2 and *drh-1* animals raise a small RNA response to VSV-dsRED infection but that *drh-1* animals may be impaired in generating antisense small RNAs.

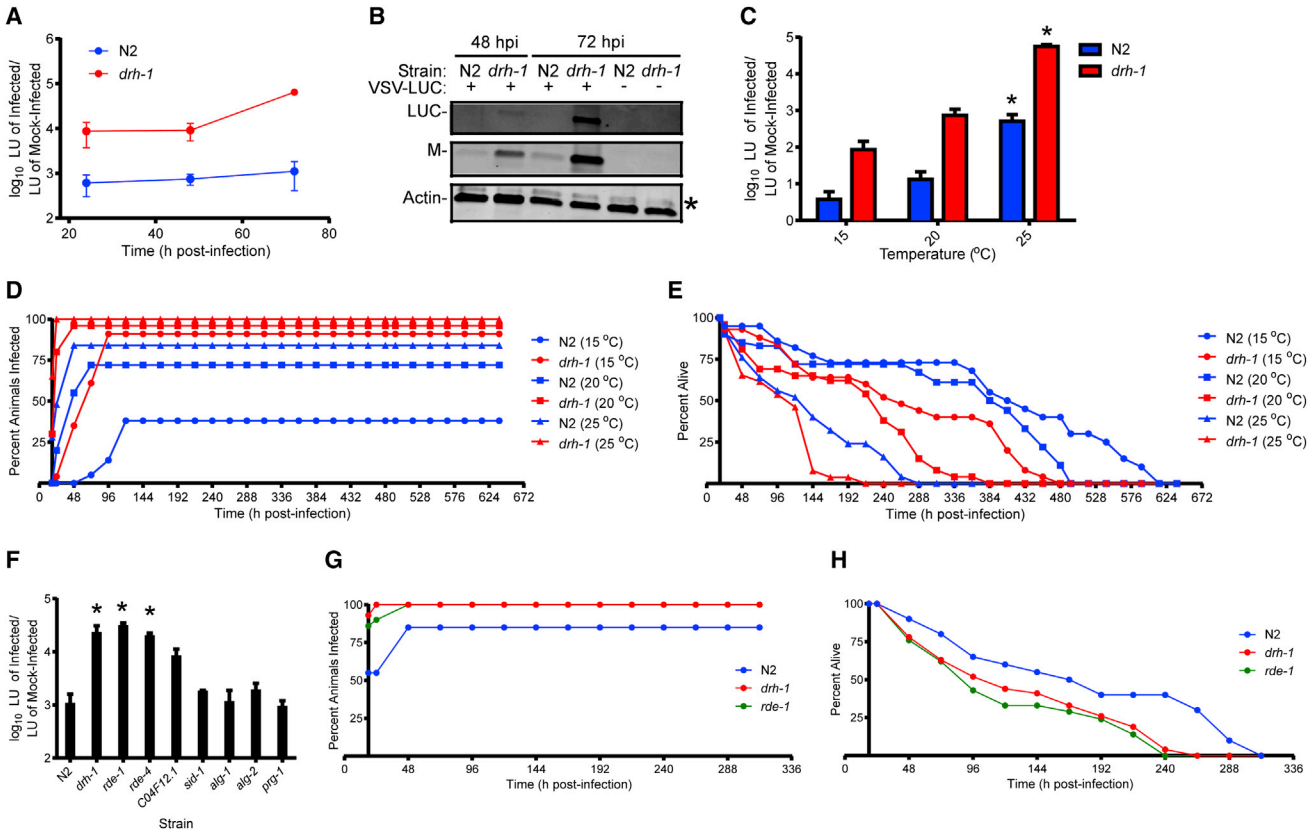

Figure 4. Characterization of the Effects of Nematode Culturing Temperature and Host Genetic Background on VSV Replication and Host Survival

(A) Luciferase (LUC) assay (in arbitrary light units, LUs) of adult animals (n = 15/treatment/experiment) infected with 10^4 PFU of VSV-LUC. LUs detected from infected animals were divided by the LUs obtained from mock-infected animals of the same strain. Data represent means (±SEM).

(B) Immunoblot of lysates from (A) for LUC, VSV Matrix (M), and cellular actin proteins. The asterisk indicates a non-specific band in the actin immunoblot.

(C) LUC assay of lysates from adult animals (n = 10/treatment/experiment) infected with 10^4 PFU of VSV-LUC and cultured at the indicated temperatures until 72 hpi. Data represent means (±SEM), and asterisks indicate treatments that are significantly different ($p < 0.05$) from 15°C treatments within strains.

(D) Percentage of animals (n = 20–30/treatment) displaying dsRED signal at the indicated times post-infection with 10^4 PFU of VSV-dsRED.

(E) Percentage of animals from (D) alive at the indicated times post-infection.

(F) LUC assay of lysates from adult animals (n = 10/treatment/experiment) infected with 10^4 PFU of VSV-LUC until 72 hpi. LUs detected from infected animals were divided by LUs obtained from mock-infected N2 animals. Data represent means (±SEM), and asterisks indicate treatments that are significantly different ($p < 0.05$) from N2 treatments.

(G) Percentage of animals (n = 20–30/treatment) displaying dsRED signal at the indicated times post-infection with 10^4 PFU of VSV-dsRED.

(H) Percentage of animals from (G) alive at the indicated times post-infection.

Development of a Luciferase Assay for VSV Replication in *C. elegans*

To further characterize VSV infection dynamics, we created a simple, quantitative assay to assess VSV replication. To do this, we employed a recombinant VSV strain encoding a firefly luciferase (LUC) gene under a viral promoter (VSV-LUC [25]) along with chemiluminescent LUC assays to measure VSV gene expression. LUC activity detected from VSV-LUC infections closely mirrors virion production and serves as a convenient and sensitive assay for virus production [24]. To test the utility of these assays, we microinjected groups of N2 or *drh-1* animals with VSV-LUC and collected equal numbers of animals at various times post-infection. Although light unit (LU) signals from infected N2 animals were ~600-fold higher than from mock-infected animals by 24 hpi, these signals only increased by ~2-fold by 72 hpi (Figure 4A). In contrast, LU signals from VSV-LUC-infected *drh-1* animals were ~8,800-fold higher than from mock-infected animals by 24 hpi and these signals increased by ~7-fold by 72 hpi. Trends observed in LUC assays were further confirmed by immunoblotting (Figure 4B). Although we were unable to detect LUC protein from infected N2 lysates, we did detect a small amount of VSV Matrix structural protein (Figure 4B). In contrast, abundant LUC and Matrix proteins were detected in VSV-LUC-infected *drh-1* lysates (Figure 4B). Collectively, these data show that LUC assays provide a sensitive and convenient method to assess VSV replication in *C. elegans*.

VSV Replication and Infection and Mortality Rates Are Temperature Dependent

To determine whether temperature influences VSV replication, we measured LU signals from VSV-LUC-infected animals

cultured at 15°C, 20°C, or 25°C. LU signals were significantly higher when either N2 or *drh-1* animals were cultured at 25°C as compared to 15°C ($p < 0.05$). Although not statistically different, LU signals from 20°C incubations trended toward being higher than signals from 15°C incubations (Figure 4C).

To investigate whether temperature affected infection or mortality rates, we challenged animals with VSV-dsRED and then monitored animals for infection (Figure 4D) and survival (Figure 4E). Interestingly, incubation temperatures appeared to affect both the maximum percentage of animals infected and the timing of when these values were reached. For example, use of 15°C, 20°C, and 25°C incubation temperatures resulted in maximal infection rates of 38%, 72%, and 84% of N2 animals by 120, 72, and 48 hpi, respectively (Figure 4D). A similar trend was observed for *drh-1* animals (albeit with higher infection rates) such that 91%, 95%, and 100% of animals incubated at 15°C, 20°C, and 25°C scored as infected by 96, 48, and 24 hpi, respectively (Figure 4D).

Examination of survival rates suggested that LT_{50} values decrease with increasing temperature (Figure 4E). For example, LT_{50} (95% CI) values for infected N2 animals cultured at 15°C (408 hpi [403–413 hpi]), 20°C (384 hpi [380–388 hpi]), and 25°C (124 hpi [116–131 hpi]) were all significantly different from one another. The LT_{50} (95% CI) values for infected *drh-1* animals cultured at 15°C (257 hpi [239–274 hpi]), 20°C (191 hpi [177–205 hpi]), and 25°C (94 hpi [86–101 hpi]) also decreased with increasing temperature. Collectively, these results suggest that VSV replication and infection rates increase with increasing temperature, whereas animal survival rates decrease.

Downstream Components of the Antiviral RNAi Pathway Are Also Required to Restrict VSV Infection

We next wanted to examine whether strains with loss-of-function mutations in other RNAi pathway components display VSV hypersusceptibility. Using our LUC-based assays for viral replication, we found that, in addition to *drh-1* animals, the RNAi-defective strains *rde-1* [26] and *rde-4* [26] also displayed significantly higher ($p < 0.05$) VSV-LUC replication than N2 animals (Figure 4F), suggesting that these downstream components are also required to restrict viral replication. Although LU signals in RNAi-defective *C04F12.1* mutants [27] were ~8-fold higher than in N2 animals, these values did not reach statistical significance ($p = 0.1$). Furthermore, strains deficient for SID-1 (required for systemic spreading of exogenous RNAi signals [28]), ALG-1 and ALG-2 (Argonautes involved in the microRNA pathway [29]), and PRG-1 (an Argonaute required for the Piwi-interacting RNA pathway [30]) did not display altered VSV-LUC susceptibilities ($p > 0.05$).

We next asked whether the enhanced viral replication observed in *rde-1* animals correlated with increased infection rates and reduced survival rates. Whereas only 85% of N2 animals scored positive for infection, all *drh-1* and *rde-1* animals displayed dsRED signal by 48 hpi (Figure 4G). Furthermore, the LT_{50} (95% CI) values for both *drh-1* (119 hpi [105–133 hpi]) and *rde-1* (105 hpi [90–121 hpi]) animals were significantly lower than that of N2 animals (168 hpi [164–172 hpi]) but did not significantly differ from one another (Figure 4H). These data suggest that RNAi pathway components downstream of DRH-1 are also required for combating VSV infection.

DRH-1 Is Required for Full Immunity to Vertical Virus Transmission

During our lifespan assays, we noticed that when we used nematode growth medium (NGM) plates containing the DNA synthesis inhibitor fluorodeoxyuridine (FUdR), dsRED-positive embryos could often be observed with a fluorescence stereo zoom microscope on plates containing VSV-dsRED-infected *drh-1* animals (Figure 5A). FUdR has been shown to induce sterility and prevent egg hatching [31], and thus is useful when tracking adult nematodes over extended incubation periods. Importantly, FUdR does not impede VSV replication [32], and thus is not expected to directly affect viral replication. We further confirmed dsRED signals in embryos using differential interference contrast and fluorescence microscopy (Figure 5B). Furthermore, dsRED signals could be observed in oocytes (Figure S4A) and embryos (Figure S4B) within infected *drh-1* animals, suggesting that VSV-dsRED was entering and infecting germline tissues. We further confirmed VSV transcription in dsRED-positive embryos using RT-PCR (Figure S5).

Given our inability to detect dsRED-positive embryos in our initial experiments using normal NGM plates, we asked whether FUdR treatment might influence vertical transmission of VSV-dsRED. When cultured on control plates, both mock- and VSV-dsRED-infected N2 and *drh-1* animals produced a similar number of total progeny, suggesting that there were no virus- or strain-dependent differences. Similar results were obtained when injected animals were cultured on FUdR plates, albeit the total progeny sizes were reduced compared to control plates and a greater proportion of progeny were embryos (Figure 5C). Despite these reduced brood sizes, dsRED-positive embryos were only detected on FUdR plates containing *drh-1* animals (Figure 5D). Because only ~9% of embryos laid by infected *drh-1* animals displayed dsRED signal, we wanted to confirm that this was not simply a "jackpot" event that only occurred on *drh-1* plates by chance. Therefore, we repeated these experiments using larger numbers of N2 and *drh-1* adults and plated all VSV-dsRED-infected animals onto FUdR plates. Despite similar brood sizes between N2 and *drh-1* strains (Figure 5E), dsRED-positive embryos were again only detected on *drh-1* plates (Figure 5F).

We next asked whether direct germline injection of VSV-dsRED might alter either overall or germline tissue-specific infection rates in N2 or *drh-1* animals after culturing animals on FUdR. Interestingly, both strains displayed similar overall infection rates when challenged by either somatic or germline VSV-dsRED injections. In contrast, higher germline infection rates were observed when VSV-dsRED was directly injected into the germline (as oppose to the soma) for both N2 (0% versus 6%) and *drh-1* (24% versus 74%) animals (Figure S6A). These data suggest that direct injection of VSV-dsRED particles into the germline may overwhelm germline antiviral defenses that might otherwise be protective when VSV-dsRED must first spread from somatic tissues.

We next asked whether FUdR was still required to observe germline VSV-dsRED infection after direct challenge of the germline of *drh-1* animals. Strikingly, we observed similar germline infection rates in animals cultured on either control or FUdR-containing medium (Figure S6B). These data suggest that FUdR does not influence germline infection rates when VSV-dsRED is directly injected into the germline.

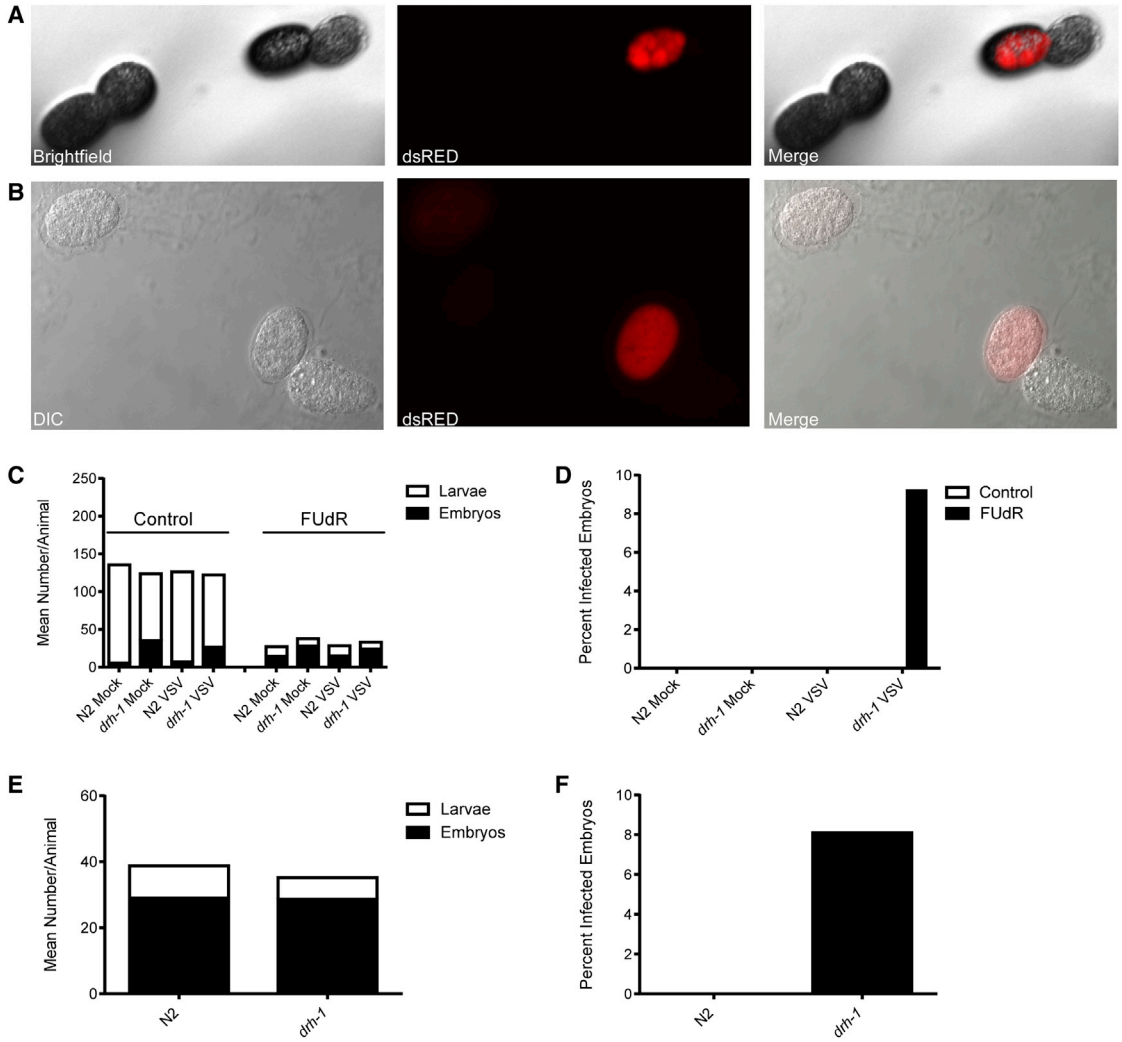

Figure 5. DRH-1 Is Required for Full Immunity to Vertical Virus Transmission

(A) Bright-field and fluorescence micrographs (112× magnification) taken with a fluorescence stereo zoom microscope of a dsRED-positive embryo laid by an adult *drh-1* animal infected with VSV-dsRED.

(B) DIC and fluorescence micrographs (40× magnification) of dsRED-positive embryos laid by an adult *drh-1* animal infected with VSV-dsRED.

(C) Mean number (±SEM) of larvae or dead embryos laid by mock- or VSV-dsRED-infected animals (n = 10 animals/treatment) 48 hpi when cultured on normal nematode growth media (control) or media containing fluorodeoxyuridine (FUdR).

(D) Percentage of total embryos from (C) displaying dsRED signal.

(E) Mean number (±SEM) of larvae or dead embryos laid by VSV-dsRED-infected animals (n = 20 animals/treatment) 48 hpi when cultured on plates containing FUdR.

(F) Percentage of total embryos from (E) displaying dsRED signal.

See also Figures S4–S6.

Collectively, these results show that VSV can be vertically transmitted to offspring, and that germline immunity to VSV infection can be influenced by the site of injection, the presence of FUdR in the culturing medium, and DRH-1 function.

Inheritance of Antiviral Immunity after VSV Infection

Although there is clear evidence for the transgenerational inheritance of RNAi responses generated by expression of foreign transgenes or the flock house virus replicon in *C. elegans* [33, 34], inheritance of antiviral RNAi responses to OV remains controversial. Therefore, we were interested to determine whether transgenerational immunity could be observed with our VSV model. To address this, we collected embryos from N2 animals that had either been mock or VSV-dsRED infected, allowed the resultant progeny to develop to adulthood, and then challenged these progeny with VSV-dsRED. As shown in Figure 6A, animals whose mother was previously exposed to VSV-dsRED exhibited a significantly lower infection rate than animals whose mother had been mock infected ($p < 0.01$). We then asked whether this inherited protection against infection could also be observed in *drh-1* animals. Interestingly, we found that both N2 and *drh-1* progeny animals displayed significantly

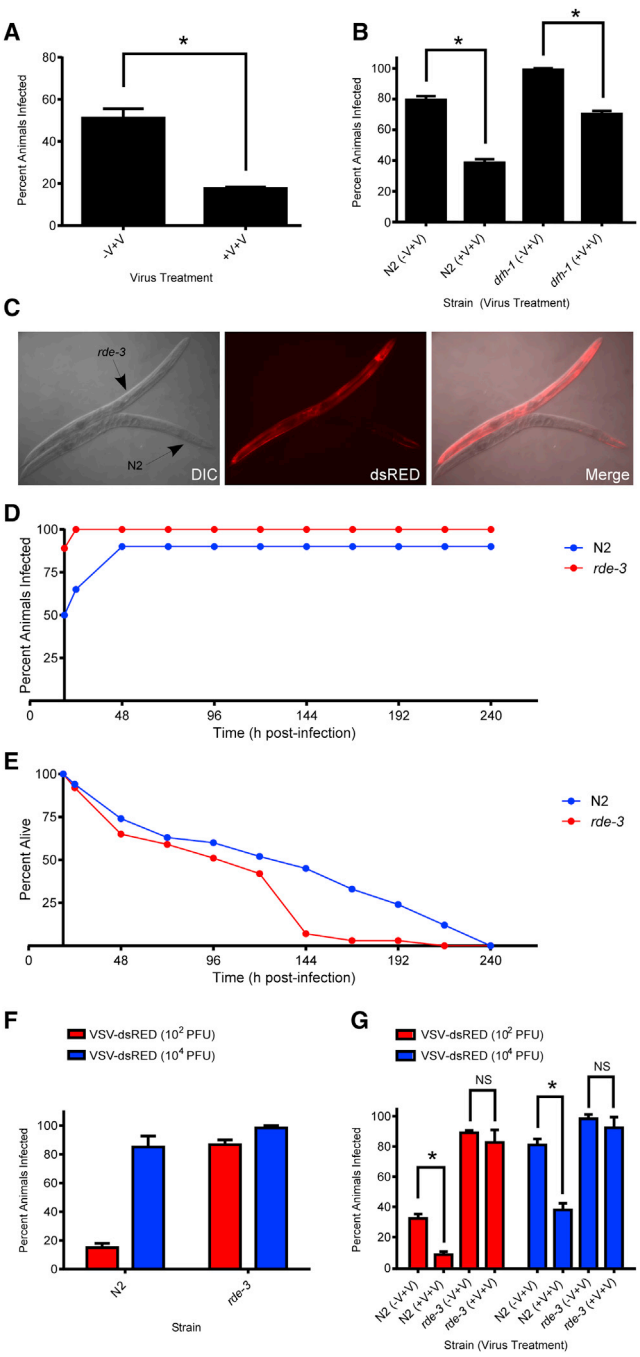

Figure 6. Prior Exposure of Parental Animals to Virus Infection Confers Protective Immunity to Their Progeny that Is Dependent on RDE-3

(A) Percentage of progeny animals collected from mock- (−V+V) or VSV-dsRED-infected (+V+V) mothers displaying dsRED signal 96 hpi with 10^3 PFU of VSV-dsRED.

(B) Percentage of N2 or *drh-1* progeny animals collected from mock- (−V+V) or VSV-dsRED-infected (+V+V) mothers displaying dsRED signal 72 hpi with 10^4 PFU of VSV-dsRED.

(C) DIC and fluorescence micrographs (10× magnification) of N2 or *rde-3* adults infected with 10^4 PFU of VSV-dsRED. Images were taken 72 hpi.

(D) Percentage of animals displaying dsRED signal at the indicated times post-infection with 10^4 PFU of VSV-dsRED.

(E) Percentage of animals from (D) alive at the indicated times post-infection.

(F) Percentage of N2 or *rde-3* animals displaying dsRED signal at 72 hpi after challenge with the indicated doses of VSV-dsRED.

(G) Percentage of N2 or *rde-3* progeny animals collected from mock- (−V+V) or VSV-dsRED-infected (+V+V) mothers displaying dsRED signal 72 hpi after challenge with either 10^2 or 10^4 PFU of VSV-dsRED.

All quantitative experiments used 20–30 animals/treatment and data in bar graphs represent means (±SEM). Where statistical analyses were performed, asterisks indicate treatments that are significantly different ($p < 0.05$) from control (−V+V) treatments. NS, not significant.

reduced infection rates when they derived from infected mothers as opposed to mock-infected mothers ($p < 0.05$) (Figure 6B).

In *C. elegans*, heritable antiviral immunity is thought to be mediated by small RNAs [34, 35], and our deep-sequencing results revealed a reduced, but not absent, small RNA response against VSV-dsRED in *drh-1* animals. Therefore, we thought it possible that the residual small RNA response (consisting primarily of 22Gs) in *drh-1* animals might still be capable of mediating a protective effect in resulting progeny. To address this, we made use of animals with an inactivating mutation in the *rde-3* gene, which encodes a putative nucleotidyl transferase required for 22G biogenesis [36, 37]. When challenged with 10^4 PFU of VSV-dsRED, *rde-3* animals displayed hypersusceptibility to infection as evidenced by infection of multiple tissues (Figure 6C), elevated infection rates (Figure 6D), and significantly reduced LT_{50} (91 versus 123 hpi) values compared to N2 animals (Figure 6E). Higher infection rates of *rde-3* animals were not only observed with higher doses (10^4 PFU) but also at lower doses (10^2 PFU), further confirming the hypersusceptibility of *rde-3* animals to infection (Figure 6F). We then performed transgenerational immunity assays with N2 and *rde-3* animals in which progeny from mock- or VSV-dsRED-infected mothers were challenged with either 10^2 or 10^4 PFU of VSV-dsRED and then scored for infection 72 hr later. Whereas N2 progeny derived from infected mothers displayed significantly reduced infection rates compared to those from mock-infected mothers when challenged with either low or high viral doses ($p < 0.05$), this protective effect was lost in *rde-3* animals ($p > 0.05$) (Figure 6G). Collectively, our results suggest that VSV infection of adult animals can lead to a heritable antiviral response that is dependent upon RDE-3 function.

DISCUSSION

The advantages of using VSV-dsRED microinjection for viral studies in *C. elegans* are that it allows the direct delivery of a known quantity of virus into an animal as well as the ability to score for infection and tissue involvement in real time. The infection of RNAi-deficient mutants has revealed the ability of VSV to replicate not only in muscle tissue (as in N2 infections) but also in various tissues throughout the animal. The muscle-tropic nature of N2 infections was surprising given that in mouse models, VSV is typically neurotropic, although other tissues, including muscle, can become involved [19]. VSV neurotropism in mice might reflect tissue-specific differences in antiviral responses [19], and so it is possible that in *C. elegans*, muscle tissue antiviral responses may be less robust than in other tissues.

Although previous studies have reported enhanced nodavirus replication in animals defective for RNAi pathway components

such as DRH-1 [9, 13], RDE-1 [14], and RDE-4 [14], it was unclear whether these factors contributed to the restriction of negative-sense ssRNA virus infection in vivo. A mammalian homolog of DRH-1, RIG-I, is required to initiate an interferon response to VSV infection in vertebrates [38]. The enhanced susceptibility of *drh-1* animals to VSV suggests that DRH-1 may act in an analogous manner but instead initiate an antiviral response through the RNAi pathway. Our examination of small RNA responses in VSV-infected nematodes revealed a clear reduction in antisense 22Gs targeting VSV in *drh-1* mutants compared to N2 animals. A reduction in antisense 22Gs has also been described during OV infection of *drh-1* animals, suggesting that small RNAs targeting viral transcripts contribute significantly to the restriction of virus replication [9]. Interestingly, in both N2 and *drh-1* animals there were clear "hotspots" of small RNAs mapping to the 5′ end of the VSV genome. This has also been observed during small RNA responses against VSV in *Drosophila*, and has been attributed to the presence of self-complementary snapback defective interfering particles derived from the 5′ end of the genome [39]. Curiously, although *Drosophila* Dicer proteins cleave these VSV snapback particles, the resulting siRNAs are, for unknown reasons, not loaded into Argonautes [39]. It has been postulated that these interfering particles may serve as an RNA decoy, allowing VSV evasion of RNAi machinery [39, 40]. It will be interesting to determine whether VSV produces defective interfering particles in *C. elegans* and whether small RNAs targeting these particles are loaded into RDE-1.

Although SID-1 is required for the systemic spread of exogenous RNAi signals [28], *sid-1* mutants were as susceptible to VSV as N2 animals. This is consistent with previous virus studies in *C. elegans* [3, 33]. Whether another, unidentified, RNA transporter is required for mounting systemic RNAi responses to infection is unknown.

Interestingly, we found that VSV could infect the germline of *drh-1* animals and be vertically transmitted when somatically injected animals were placed on FUdR-containing plates. How this DNA synthesis inhibitor might compromise germline immunity to infection is unknown. However, FUdR treatment can modulate resistance to thermal, hypertonic, and proteotoxic stresses, most likely through alteration of gene expression [40]. Therefore, FUdR-induced inhibition of germline gene expression programs and/or stress responses that normally serve antiviral roles may promote germline infection and vertical transmission. However, because VSV could efficiently establish germline infection after direct injection into the germline in the absence of FUdR, these drug-induced effects may only be required to sensitize the germline to infection as the virus spreads from the soma. Direct injection of VSV into the germline may simply overwhelm germline antiviral responses, even without modulation by FUdR treatment. Importantly, no evidence was found for vertical transmission of other intracellular *C. elegans* pathogens such as microsporida [41] and OV [14]. Therefore, our model provides new opportunities to study vertical transmission in *C. elegans*.

Previous reports have demonstrated that administration of a mild stress (e.g., temporary starvation) to *C. elegans* can lead to enhanced protection of offspring from these same stressors, a phenomenon termed "transgenerational hormesis" [42, 43]. In some cases, this phenomenon can be mediated by small RNAs [43]. A previous report found transgenerational silencing of a flock house virus transgene [34], and Sterken et al. [35] reported that OV-infected N2, but not RNAi-deficient, animals could transmit a heritable, protective antiviral response to their progeny. In contrast, Ashe et al. [33] did not find evidence for transgenerational immunity after OV infection. We found that prior exposure of N2 or *drh-1* animals to VSV led to significant reductions in the infection rates of their progeny when challenged with VSV. We were initially surprised by the inheritance of an antiviral response in *drh-1* animals, which is in contradiction with Sterken et al. [35]. However, because antiviral small RNA production in *drh-1* animals was reduced, but not eliminated, it is possible that these residual small RNAs may still confer protection to offspring. We attempted to detect small RNAs targeting VSV in the progeny from naive or VSV-exposed mothers but were unable to observe significant quantities of viral small RNAs in these deep-sequencing experiments. It is unclear whether viral small RNAs exist in progeny animals at too low a level for detection by our methods or whether the heritable antiviral effect is not mediated by small RNAs. We favor the former scenario, as *rde-3* animals are completely defective in 22G biogenesis [37], and we found no evidence for transgenerational antiviral immunity in *rde-3* animals. The ability of *C. elegans* to use a heritable antiviral response to protect offspring from infection represents a fascinating adaptation that warrants further investigation.

The susceptibility of *C. elegans* to VSV provides a genetically tractable in vivo model system to explore negative-sense ssRNA virus biology and antiviral immunity. Our system will nicely complement in vivo models that have been established for VSV in *Drosophila* and mice [19], giving investigators the rare opportunity to study a single virus in disparate hosts.

EXPERIMENTAL PROCEDURES

Cell, Virus, and Worm Culture

Baby hamster kidney (BHK) and BSC-40 cells (American Type Culture Collection) were cultured as described [24] in Dulbecco's modified Eagle's medium (DMEM; Invitrogen). VSV stocks were prepared as described [24] and resuspended in DMEM. Viral and nematode strains used in the study are described in the Supplemental Experimental Procedures. Unless otherwise indicated, NGM plates were incubated at 25°C for the duration of experiments.

Microinjections

Microinjections used young adults and pulled capillary needles secured onto a Nikon TE200 microscope equipped with a micromanipulator and regulated pressure source. Needles containing either DMEM (mock infections) or virus resuspended in DMEM were used for microinjections. Doses of VSV (in PFU) represent estimates based on VSV titration of BSC-40 cells and a dispensed volume of 10 nL during microinjections. Injected worms were immediately placed on NGM plates seeded with OP50 *Escherichia coli*. Where indicated, NGM also contained 50 μg/mL FUdR (Sigma).

RNA Isolation and RT-PCR

Total RNA was purified from adult worms or embryos at the indicated times as described [44]. VSV (+)-sense transcription and *C. elegans* actin gene transcription were analyzed by RT-PCR as described [24].

Immunoblotting

Antibodies used for immunoblotting included mouse anti-LUC (Invitrogen), rabbit anti-actin (Abcam), and mouse anti-VSV Matrix (Douglas Lyles, Wake Forest School of Medicine). Immunoblots were performed as described [24].

Lifespan, LUC, and Transgenerational Immunity Assays, Microscopy, and Small RNA Cloning and Analysis
See the Supplemental Experimental Procedures for details.

SUPPLEMENTAL INFORMATION

Supplemental Information includes Supplemental Experimental Procedures and six figures and can be found with this article online at http://dx.doi.org/10.1016/j.cub.2017.02.004.

AUTHOR CONTRIBUTIONS

Conception and design: D.B.G., T.I., W.G., N.S., C.C.M. Acquisition of data: D.B.G., T.I., L.L. Analysis and interpretation of data: D.B.G., T.I., L.L., W.G., N.S., C.C.M. Drafting or revision of the article: D.B.G., T.I., L.L., W.G., N.S., C.C.M.

ACKNOWLEDGMENTS

We thank Dr. Rita Sharma and Ms. Tauny Tambolleo for excellent technical assistance. D.B.G. was supported by fellowships from the Natural Sciences and Engineering Research Council of Canada and Alberta Innovates Health Solutions. C.C.M. was funded by the NIH (grant 5R37GM058800) and is a Howard Hughes Medical Institute Investigator. N.S. was funded by the NIH (grant AI060025).

Received: November 14, 2016
Revised: January 18, 2017
Accepted: February 1, 2017
Published: March 2, 2017

REFERENCES

1. Zhang, R., and Hou, A. (2013). Host-microbe interactions in *Caenorhabditis elegans*. ISRN Microbiol. *2013*, 356451.
2. Cohen, L.B., and Troemel, E.R. (2015). Microbial pathogenesis and host defense in the nematode *C. elegans*. Curr. Opin. Microbiol. *23*, 94–101.
3. Schott, D.H., Cureton, D.K., Whelan, S.P., and Hunter, C.P. (2005). An antiviral role for the RNA interference machinery in *Caenorhabditis elegans*. Proc. Natl. Acad. Sci. USA *102*, 18420–18424.
4. Wilkins, C., Dishongh, R., Moore, S.C., Whitt, M.A., Chow, M., and Machaca, K. (2005). RNA interference is an antiviral defence mechanism in *Caenorhabditis elegans*. Nature *436*, 1044–1047.
5. Gammon, D.B., and Mello, C.C. (2015). RNA interference-mediated antiviral defense in insects. Curr. Opin. Insect Sci. *8*, 111–120.
6. Szittya, G., and Burgyán, J. (2013). RNA interference-mediated intrinsic antiviral immunity in plants. Curr. Top. Microbiol. Immunol. *371*, 153–181.
7. Maillard, P.V., Ciaudo, C., Marchais, A., Li, Y., Jay, F., Ding, S.W., and Voinnet, O. (2013). Antiviral RNA interference in mammalian cells. Science *342*, 235–238.
8. Li, Y., Lu, J., Han, Y., Fan, X., and Ding, S.W. (2013). RNA interference functions as an antiviral immunity mechanism in mammals. Science *342*, 231–234.
9. Ashe, A., Bélicard, T., Le Pen, J., Sarkies, P., Frézal, L., Lehrbach, N.J., Félix, M.A., and Miska, E.A. (2013). A deletion polymorphism in the *Caenorhabditis elegans* RIG-I homolog disables viral RNA dicing and antiviral immunity. eLife *2*, e00994.
10. Pak, J., and Fire, A. (2007). Distinct populations of primary and secondary effectors during RNAi in *C. elegans*. Science *315*, 241–244.
11. Sijen, T., Steiner, F.A., Thijssen, K.L., and Plasterk, R.H. (2007). Secondary siRNAs result from unprimed RNA synthesis and form a distinct class. Science *315*, 244–247.
12. Lu, R., Maduro, M., Li, F., Li, H.W., Broitman-Maduro, G., Li, W.X., and Ding, S.W. (2005). Animal virus replication and RNAi-mediated antiviral silencing in *Caenorhabditis elegans*. Nature *436*, 1040–1043.
13. Lu, R., Yigit, E., Li, W.X., and Ding, S.W. (2009). An RIG-I-like RNA helicase mediates antiviral RNAi downstream of viral siRNA biogenesis in *Caenorhabditis elegans*. PLoS Pathog. *5*, e1000286.
14. Félix, M.A., Ashe, A., Piffaretti, J., Wu, G., Nuez, I., Bélicard, T., Jiang, Y., Zhao, G., Franz, C.J., Goldstein, L.D., et al. (2011). Natural and experimental infection of *Caenorhabditis* nematodes by novel viruses related to nodaviruses. PLoS Biol. *9*, e1000586.
15. Franz, C.J., Renshaw, H., Frezal, L., Jiang, Y., Félix, M.A., and Wang, D. (2014). Orsay, Santeuil and Le Blanc viruses primarily infect intestinal cells in *Caenorhabditis* nematodes. Virology *448*, 255–264.
16. Whelan, S.P., Ball, L.A., Barr, J.N., and Wertz, G.T. (1995). Efficient recovery of infectious vesicular stomatitis virus entirely from cDNA clones. Proc. Natl. Acad. Sci. USA *92*, 8388–8392.
17. Lawson, N.D., Stillman, E.A., Whitt, M.A., and Rose, J.K. (1995). Recombinant vesicular stomatitis viruses from DNA. Proc. Natl. Acad. Sci. USA *92*, 4477–4481.
18. Liang, G., Gao, X., and Gould, E.A. (2015). Factors responsible for the emergence of arboviruses; strategies, challenges and limitations for their control. Emerg. Microbes Infect. *4*, e18.
19. Hastie, E., Cataldi, M., Marriott, I., and Grdzelishvili, V.Z. (2013). Understanding and altering cell tropism of vesicular stomatitis virus. Virus Res. *176*, 16–32.
20. Duntsch, C.D., Zhou, Q., Jayakar, H.R., Weimar, J.D., Robertson, J.H., Pfeffer, L.M., Wang, L., Xiang, Z., and Whitt, M.A. (2004). Recombinant vesicular stomatitis virus vectors as oncolytic agents in the treatment of high-grade gliomas in an organotypic brain tissue slice-glioma coculture model. J. Neurosurg. *100*, 1049–1059.
21. Kern, A., Ackermann, B., Clement, A.M., Duerk, H., and Behl, C. (2010). HSF1-controlled and age-associated chaperone capacity in neurons and muscle cells of *C. elegans*. PLoS ONE *5*, e8568.
22. Guo, X., Zhang, R., Wang, J., Ding, S.W., and Lu, R. (2013). Homologous RIG-I-like helicase proteins direct RNAi-mediated antiviral immunity in *C. elegans* by distinct mechanisms. Proc. Natl. Acad. Sci. USA *110*, 16085–16090.
23. Roers, A., Hiller, B., and Hornung, V. (2016). Recognition of endogenous nucleic acids by the innate immune system. Immunity *44*, 739–754.
24. Gammon, D.B., Duraffour, S., Rozelle, D.K., Hehnly, H., Sharma, R., Sparks, M.E., West, C.C., Chen, Y., Moresco, J.J., Andrei, G., et al. (2014). A single vertebrate DNA virus protein disarms invertebrate immunity to RNA virus infection. eLife *3*, e02910.
25. Cureton, D.K., Massol, R.H., Saffarian, S., Kirchhausen, T.L., and Whelan, S.P. (2009). Vesicular stomatitis virus enters cells through vesicles incompletely coated with clathrin that depend upon actin for internalization. PLoS Pathog. *5*, e1000394.
26. Tabara, H., Sarkissian, M., Kelly, W.G., Fleenor, J., Grishok, A., Timmons, L., Fire, A., and Mello, C.C. (1999). The rde-1 gene, RNA interference, and transposon silencing in *C. elegans*. Cell *99*, 123–132.
27. Kim, J.K., Gabel, H.W., Kamath, R.S., Tewari, M., Pasquinelli, A., Rual, J.F., Kennedy, S., Dybbs, M., Bertin, N., Kaplan, J.M., et al. (2005). Functional genomic analysis of RNA interference in *C. elegans*. Science *308*, 1164–1167.
28. Winston, W.M., Molodowitch, C., and Hunter, C.P. (2002). Systemic RNAi in *C. elegans* requires the putative transmembrane protein SID-1. Science *295*, 2456–2459.
29. Grishok, A., Pasquinelli, A.E., Conte, D., Li, N., Parrish, S., Ha, I., Baillie, D.L., Fire, A., Ruvkun, G., and Mello, C.C. (2001). Genes and mechanisms related to RNA interference regulate expression of the small temporal RNAs that control *C. elegans* developmental timing. Cell *106*, 23–34.
30. Batista, P.J., Ruby, J.G., Claycomb, J.M., Chiang, R., Fahlgren, N., Kasschau, K.D., Chaves, D.A., Gu, W., Vasale, J.J., Duan, S., et al. (2008). PRG-1 and 21U-RNAs interact to form the piRNA complex required for fertility in *C. elegans*. Mol. Cell *31*, 67–78.

31. Mitchell, D.H., Stiles, J.W., Santelli, J., and Sanadi, D.R. (1979). Synchronous growth and aging of *Caenorhabditis elegans* in the presence of fluorodeoxyuridine. J. Gerontol. *34*, 28–36.
32. Levine, S., and Olson, W. (1963). Nucleic acids of measles and vesicular stomatitis viruses. Proc. Soc. Exp. Biol. Med. *113*, 630–631.
33. Ashe, A., Sarkies, P., Le Pen, J., Tanguy, M., and Miska, E.A. (2015). Antiviral RNA interference against Orsay virus is neither systemic nor transgenerational in *Caenorhabditis elegans*. J. Virol. *89*, 12035–12046.
34. Rechavi, O., Minevich, G., and Hobert, O. (2011). Transgenerational inheritance of an acquired small RNA-based antiviral response in *C. elegans*. Cell *147*, 1248–1256.
35. Sterken, M.G., Snoek, L.B., Bosman, K.J., Daamen, J., Riksen, J.A., Bakker, J., Pijlman, G.P., and Kammenga, J.E. (2014). A heritable antiviral RNAi response limits Orsay virus infection in *Caenorhabditis elegans* N2. PLoS ONE *9*, e89760.
36. Chen, C.C., Simard, M.J., Tabara, H., Brownell, D.R., McCollough, J.A., and Mello, C.C. (2005). A member of the polymerase beta nucleotidyltransferase superfamily is required for RNA interference in *C. elegans*. Curr. Biol. *15*, 378–383.
37. Shirayama, M., Seth, M., Lee, H.C., Gu, W., Ishidate, T., Conte, D., Jr., and Mello, C.C. (2012). piRNAs initiate an epigenetic memory of nonself RNA in the *C. elegans* germline. Cell *150*, 65–77.
38. Kato, H., Takeuchi, O., Sato, S., Yoneyama, M., Yamamoto, M., Matsui, K., Uematsu, S., Jung, A., Kawai, T., Ishii, K.J., et al. (2006). Differential roles of MDA5 and RIG-I helicases in the recognition of RNA viruses. Nature *441*, 101–105.
39. Sabin, L.R., Zheng, Q., Thekkat, P., Yang, J., Hannon, G.J., Gregory, B.D., Tudor, M., and Cherry, S. (2013). Dicer-2 processes diverse viral RNA species. PLoS ONE *8*, e55458.
40. Anderson, E.N., Corkins, M.E., Li, J.C., Singh, K., Parsons, S., Tucey, T.M., Sorkaç, A., Huang, H., Dimitriadi, M., Sinclair, D.A., and Hart, A.C. (2016). *C. elegans* lifespan extension by osmotic stress requires FUdR, base excision repair, FOXO, and sirtuins. Mech. Ageing Dev. *154*, 30–42.
41. Troemel, E.R., Félix, M.A., Whiteman, N.K., Barrière, A., and Ausubel, F.M. (2008). Microsporidia are natural intracellular parasites of the nematode *Caenorhabditis elegans*. PLoS Biol. *6*, 2736–2752.
42. Jobson, M.A., Jordan, J.M., Sandrof, M.A., Hibshman, J.D., Lennox, A.L., and Baugh, L.R. (2015). Transgenerational effects of early life starvation on growth, reproduction, and stress resistance in *Caenorhabditis elegans*. Genetics *201*, 201–212.
43. Rechavi, O., Houri-Ze'evi, L., Anava, S., Goh, W.S., Kerk, S.Y., Hannon, G.J., and Hobert, O. (2014). Starvation-induced transgenerational inheritance of small RNAs in *C. elegans*. Cell *158*, 277–287.
44. Gu, W., Shirayama, M., Conte, D., Jr., Vasale, J., Batista, P.J., Claycomb, J.M., Moresco, J.J., Youngman, E.M., Keys, J., Stoltz, M.J., et al. (2009). Distinct Argonaute-mediated 22G-RNA pathways direct genome surveillance in the *C. elegans* germline. Mol. Cell *36*, 231–244.